Osteogenic Differentiation of Human Bone Marrow Mesenchymal Stem Cells Seeded on Melt Based Chitosan Scaffolds for Bone Tissue Engineering Applications

Ana R. Costa-Pinto,*,† Vitor M. Correlo,† Paula C. Sol,† Mrinal Bhattacharya,‡ Pierre Charbord,§ Bruno Delorme,§ Rui L. Reis,† and Nuno M. Neves†

3B's Research Group, Biomaterials, Biodegradables and Biomimetics, Department of Polymer Engineering, Headquarters of the European Institute of Excellence on Tissue Engineering and Regenerative Medicine University of Minho, Avepark, S. Claúdio do Barco, 4806-909 Caldas das Taipas, Guimarães, Portugal, IBB, Institute for Biotechnology and Bioengineering, PT Government Associated Laboratory, Guimarães, Portugal, Department of Biosystems Engineering, University of Minnesota, St Paul, Minnesota 55108, and Equipe INSERM-ESPRI/EA3855, "Microenvironnement de l'Hématopoièse et Cellules Souches", Faculté de Médecine, 10 Bd Tonnellé, 37032 Tours Cedex 1, France

Received January 5, 2009; Revised Manuscript Received June 26, 2009

The purpose of this study was to evaluate the growth patterns and osteogenic differentiation of human bone marrow mesenchymal stem cells (hBMSCs) when seeded onto new biodegradable chitosan/polyester scaffolds. Scaffolds were obtained by melt blending chitosan with poly(butylene succinate) in a proportion of 50% (wt) each and further used to produce a fiber mesh scaffold. hBMSCs were seeded on those structures and cultured for 3 weeks under osteogenic conditions. Cells were able to reduce MTS and demonstrated increasing metabolic rates over time. SEM observations showed cell colonization at the surface as well as within the scaffolds. The presence of mineralized extracellular matrix (ECM) was successfully demonstrated by peaks corresponding to calcium and phosphorus elements detected in the EDS analysis. A further confirmation was obtained when carbonate and phosphate group peaks were identified in Fourier Transformed Infrared (FTIR) spectra. Moreover, by reverse transcriptase (RT)-PCR analysis, it was observed the expression of osteogenic gene markers, namely, Runt related transcription factor 2 (Runx2), type 1 collagen, bone sialoprotein (BSP), and osteocalcin. Chitosan-PBS (Ch-PBS) biodegradable scaffolds support the proliferation and osteogenic differentiation of hBMSCs cultured at their surface in vitro, enabling future in vivo testing for the development of bone tissue engineering therapies.

Introduction

Mesenchymal stem cells (MSCs) isolated from bone marrow stroma have the capacity to differentiate into cells of connective tissues, namely, into osteoblasts, chondrocytes, and adipocytes.[1−4] However, recent studies,[5] indicate that they may have a much broader differentiation potential. Accordingly, the multipotential capacity of MSCs, their accessible origin, high ex vivo expansive potential, and ethical acceptance, make these cells attractive tools for tissue engineering and cell-based therapies.

Annually, more than 2.2 million bone grafting procedures (autologous bone graft and banked bone) are performed worldwide to ensure adequate bone healing in many skeletal problems, such as nonunion fractures, cervical and lumbar spine fusion, joint arthrodesis, and revision arthroplasty.[6] Unfortunately, the gold standard of bone grafting (autologous bone) requires an extra surgery to retrieve it from the patient. This leads to an increase in surgical and recovery times. Potential complications, such as chronic pain at the donor site, infections, and eventual disability[7] can occur. Tissue engineering offers a strategy to circumvent those problems. The concept involves the use of a porous and biodegradable scaffold, allowing cells to adhere and proliferate, creating conditions for the formation of ECM-like structures.[8−10] Previous studies have shown that natural based polymers such as starch[11−18] or chitosan[19−36] have great potential for bone tissue engineering applications. The main advantages of these materials include low immunogenic potential, bioactive behavior, good interaction with host tissues, chemical versatility, and high availability in nature.[7]

Chitosan has already shown a range of properties, including its nonantigenicity[33] and cytocompatibility,[35,36] that suggest having adequate properties for bone tissue engineering applications. However, the material offers limited versatility in its processability. To overcome this problem, we propose a novel methodology to process chitosan by compounding this material with biodegradable aliphatic polyesters.[23] The blend combines the favorable biological properties of chitosan with the good mechanical properties and processability of polyesters,[23−30] leading to a chitosan based material with adjustable properties for tissue engineering applications.[27−30]

The purpose of the present work is to evaluate the performance of the developed microfiber mesh scaffolds. For that, we assess the cell adhesion, proliferation, and osteogenic differentiation of human MSCs isolated from bone marrow and seeded onto novel chitosan/polyester microfiber mesh scaffolds aimed to be used in bone tissue engineering field.

* To whom correspondence should be addressed. Tel.: +351-253-510913. Fax: +351 253-510909. E-mail: arpinto@dep.uminho.pt.
† 3B's Research Group and IBB.
‡ University of Minnesota.
§ Equipe INSERM-ESPRI/EA3855.

Materials and Methods

Scaffold Processing. New chitosan based scaffolds were, developed by a fiber bonding technique. The processing methodology is entirely

10.1021/bm9000102 CCC: $40.75
Published on Web 07/21/2009

melt based, thus avoiding the limitations of solvent-based processing, and it is described in detail elsewhere.[23] Briefly, chitosan was melt blended with polybutylene succinate (PBS; 50/50 wt %) in a twin-screw extruder. The extrudate was grinded into powder and further processed into microfibers, using a microextruder. The diameter of the fibers was controlled by the diameter of the die. After that, Ch-PBS fibers were cut and submitted to hot compression. This last step[15] consisted in applying temperature and pressure to obtain a fiber mesh scaffold with inherent porosity and interconnectivity.

The scaffolds were sterilized by ethylene oxide and used for cell culture studies.

Scaffolds Characterization. Chitosan-based fiber mesh scaffolds were analyzed using a high-resolution microcomputed tomography Skyscan 1072 scanner (Skyscan, Kontich, Belgium). Five scaffolds were scanned in high resolution mode using a pixel size of 8.24 μm and integration time of 2.0 ms. The X-ray source was set at 80 keV of energy and 124 μA of current. For all the scanned specimens representative data sets of 150 slices were transformed into binary using a dynamic threshold of 60−255 (gray values) to distinguish polymer material from pore voids. This data was used for morphometric analysis (CT Analyzer v1.5.1.5, SkyScan). The morphometric analysis included porosity, scaffolds interconnectivity and mean pore size quantification. Three dimensional (3D) virtual models of representative regions in the bulk of the scaffolds were also created, visualized and registered using the image processing software (ANT 3D creator v2.4, SkyScan).

The mechanical properties of the scaffolds were tested on compression tests carried out in a universal tensile testing machine (Instron 4505, Universal Machine). A crosshead speed of 5 mm/min was used and the compression modulus was determined from the most linear region of the stress−strain curve and averaged from the results obtained with five specimens.

Cell Culture Studies. *In Vitro Cytotoxicity Tests.* A rat lung fibroblast cell line-L929, acquired from the European Collection of Cell Cultures (ECACC), was used for the initial standard cytotoxicity assays. Tests were carried out following the international standard ISO 10993. The procedure and methods are described elsewhere.[19]

hBMSCs Seeding and Culture onto the Scaffolds. Primary cultures of hBMSCs were used. The cells were characterized by flow cytometry for MSCs markers (CD31, CD34, CD45-negative and CD13, CD29, CD73, CD90, CD105, CD166-positive cells) and differentiation studies into osteogenic, chondrogenic, and adipogenic lineage.[37] The cells were grown in a culture medium consisting of alpha medium (Sigma, St. Louis, MO), 10% fetal bovine serum (Biochrom AG, Germany), 5 mM L-glutamine (Sigma, St. Louis, MO), 1 ng/mL basic fibroblast growth factor (bFgF; PeproTech, U.S.A.), and 1% of antibiotic-antimycotic mixture (Sigma, St. Louis, MO). When an adequate cell number was obtained, cells at passage 2 were detached with trypsin/EDTA. Cells were seeded at a density of 2.5×10^5 cells/scaffold under static conditions, by means of a cell suspension. After 24 h of attachment, cell-constructs were placed in new 24-well plates and 1 mL of osteogenic medium was added to each well. The osteogenic culture medium consisted of DMEM without phenol red, dexamethasone 10^{-8} M (Sigma, St. Louis, MO), ascorbic acid 50 μg/mL (Sigma, St. Louis, MO), and β-glycerophosphate 10 mM (Sigma, St. Louis, MO). The cell-constructs were cultured for periods of up to 7, 14, and 21 days in a humidified atmosphere at 37 °C, containing 5% CO_2.

The culture medium was changed every 2−3 days until the end of the experiment.

Cellular Viability Assay: MTS Test. Cell viability was assessed after 3 h, 7, 14, and 21 days, using the MTS test. The cell-constructs (n = 3) were rinsed three times in phosphate-buffered saline (Sigma, St. Louis, MO) and immersed in a mixture consisting of serum-free cell culture medium and MTS reagent in a 5:1 ratio and incubated for 3 h at 37 °C in a humidified atmosphere containing 5% CO_2. After this, 200 μL (n = 3) were transferred to 96-well plates and the optical density (O.D.) was measured on a microplate ELISA reader (BioTek, U.S.A.) using an absorbance of 490 nm.

Cell Adhesion and Cell Viability Stained with Calcein-AM Using Confocal Laser Microscopy. Cells were incubated with calcein AM (Molecular Probes, Invitrogen, U.S.A.). Inside the cells, calcein-AM is hydrolyzed by endogenous esterases into the highly negatively charged green fluorescent calcein, which is retained inside the cytoplasm. The cell-constructs were sectioned and cell adhesion, proliferation, and viability were observed in the inner regions of the scaffolds using an Olympus FluoView FV1000 confocal laser scanning microscope.

Cell Adhesion and Morphology by Scanning Electron Microscopy (SEM). Cell adhesion, morphology, and spatial distribution were observed by SEM. Cell-constructs were washed in 0.15 M phosphate buffered saline and fixed in 2.5% glutaraldehyde. After that, the constructs were dehydrated using a graded series of ethanol (30, 50, 70, 90, 100%) for 15 min, twice. Then, the samples were immersed in hexamethyldisilazane[38] (HDMS; Electron Microscopy Sciences, Washington, U.S.A.) and allowed to air-dry for 2 h. Afterward, the constructs were sputter coated with gold (JEOL JFC-1100) and analyzed using a Leica Cambridge S360 scanning electron microscope.

Cell Proliferation by DNA Quantification. hBMSCs proliferation on the Ch-PBS scaffolds was determined using a fluorimetric dsDNA quantification kit (PicoGreen, Molecular Probes, Invitrogen, USA). Samples collected at days 7, 14, and 21 were washed twice with a sterile phosphate buffered saline solution and transferred into 1.5 mL microtubes containing 1 mL of ultrapure water. Cell-constructs were cryopreserved at −80 °C for further analysis. Prior to DNA quantification, samples were thawed and sonicated for 15 min. Standards were prepared with concentrations ranging between 0 and 2 mg/mL. Per each well of an opaque 96-well plate were added 28.7 μL of sample (n = 3) or standard, 71.3 μL of PicoGreen solution, and 100 μL of Tris-EDTA buffer. The plate was incubated for 10 min in the dark and fluorescence was measured using an excitation wavelength of 480 nm and an emission wavelength of 528 nm.

Alkaline Phosphatase Quantification. Samples were collected as previously described. Alkaline phosphatase (ALP) activity of the scaffold/cell-constructs (n = 3) was measured by the specific conversion of *p*-nitrophenyl phosphate (pNpp) (Sigma, St. Louis, MO) into *p*-nitrophenol (pNp). The cell-constructs were thawed at room temperature and sonicated for 15 min. The enzymatic reaction was set up by mixing 100 mL of the sample with 300 mL of substrate buffer containing 1 M diethanolamine HCl (pH 9.8) and 2 mg/mL of pNpp. The solution was further incubated at 37 °C for 1 h and the reaction was stopped by the addition of a solution containing 2 M NaOH and 0.2 mM EDTA in distilled water. The O.D. was determined at 405 nm. A standard curve was made using pNp values ranging from 0 to 20 μmol/mL. The results were normalized by DNA values and expressed in μmol of pNp produced/μg ds DNA. A detailed description of the assay can be found elsewhere.[39]

Mineralization Content by Energy Dispersive Spectroscopy (EDS). The constructs were processed as described previously for SEM. The samples (n = 3) were sputter coated with carbon (JEOL JFC-1100) with the purpose of analyzing the presence of Ca and P elements at the surface by EDS with a Leica Cambridge S360 scanning electron microscope. Sputter coating with carbon avoids overlapping of signals of the coating with the elements being analyzed.

Mineralization Crystallinity by Fourier Transform Infra-Red Spectroscopy (FTIR). The cell-constructs were washed in phosphate buffered saline and fixed in 2.5% glutaraldehyde.

The samples were pressed into pellets with potassium bromide (KBr; Riedel-de Haen, Germany). The IR spectrum was measured using a FTIR spectrometer (model IRPrestige-21, Shimadzu; Germany) in the wavelength range of 4000−400 cm^{-1}.

Osteogenic Differentiation by Reverse Transcriptase PCR. Total RNA was isolated from cells with Trizol (Sigma, St Louis, U.S.A.), according to the manufacturer protocol. A NanoDrop Microspectro-

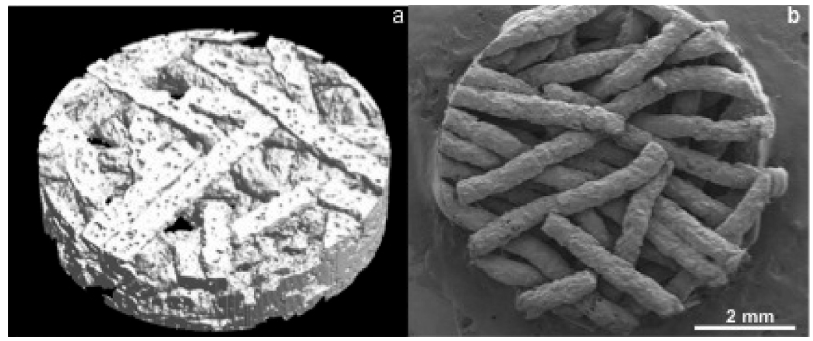

Figure 1. 3D images obtained by μ-CT reconstruction model (a) and SEM photomicrograph of Ch-PBS (50 wt %) fiber mesh scaffold (b).

photometer (NanoDrop ND-1000 Spectrophotometer, Alfagene, U.S.A.) was used to measure the total RNA amounts (ng/μL).

Aliquots of the total RNA (100 ng/μL) were transcripted into cDNA and amplified in each PCR in one step RT-PCR beads (Amersham Biosciences) and gene specific primers were added.

Each cDNA sample was run in triplicate for every PCR. Amplification was performed using a Mastercycler gradient (MyCycler, Thermal Cycler, Biorad). The first reverse transcription step at 42 °C for 30 min was followed by a step of denaturation at 95 °C during 5 min. After this, 35 cycles of PCR were performed, each consisting of a denaturation stage at 95 °C for 1 min, annealing at a given temperature accordingly with the specific primer used, and then an extension stage at 72 °C for 2 min. In all cases, a final extension at 72 °C for 5 min was performed before storing the samples at 4 °C. Specific primers used were for human Runx2, osteocalcin, type 1 collagen, BSP and for the housekeeping gene glyceraldehyde-3-phosphate dehydrogenase (GAPDH).

PCR products were separated by 1% agarose (Biorad, U.S.A.) at least twice. The separated DNA fragments were visualized by ethidium bromide (Sigma, St Louis, MO) staining and observed with an Eagleye software (Alpha Innotech, U.S.A.) using excitation at 514 nm and emission at 610 nm.

Statistical Analysis. Results of MTS and ALP are expressed as mean $\pm$ standard deviation with $n = 3$ for each group. Statistical significance of differences was determined using Student's *t*-test multiple comparison procedure at a confidence interval of 95% ($p < 0.05$).

Results

Scaffolds Characterization. Porous chitosan-based fiber mesh scaffolds used in this study were produced with a blend of 50% chitosan and 50% poly(butylene succinate). The scaffolds were prepared using melt extrusion, followed by hot compression (fiber bonding). Scaffolds were cut into cylinders of approximately 6.5 mm diameter and thickness of 1.5 mm. Figure 1 shows the top surface of the novel chitosan based fiber mesh scaffold produced by the described melt based process. Scaffolds show a large porosity and inherent interconnectivity, as well as an irregular distribution of the fiber orientation as intended.

The μ-CT technology allows obtaining series of X-ray slice images covering a representative volume region of the porous scaffold. The solid volume representation and the quantitative data is obtained following image processing using specific software and the X-rays micrographs obtained in each slice. This technique was used to obtain 3D images of the novel chitosan fiber mesh scaffolds (Figure 1a) and to quantitatively determine the average porosity (44.8% $\pm$ 2.1) and the interconnectivity of 89.6% $\pm$ 1.9. Compression mechanical tests have shown that scaffolds have a compression modulus of 32.6 $\pm$ 12.8 MPa, which is within the range of interest for bone applications.[40]

The fibers used to produce these scaffolds have an average diameter of 450 μm and as can be seen in Figure 1b, evidence an interesting surface roughness that may contribute to enhance the cell adhesion by increasing the surface area. Moreover, detailed observations using μ-CT equipment show that microfibers in addition to the surface roughness also possess some microporosity at the surface that further enhances the surface area (Figure 1a).

In Vitro Cytotoxicity Tests. In the MTS test (data not shown), L929 fibroblasts metabolized MTS into brown formazan product after incubation with the scaffold's extract. This fact evidences that the cells have metabolic activities (around 80%) similar to those obtained by cells grown in DMEM (negative control). Moreover, they were able to incorporate and metabolize MTS, showing very high viability. Therefore, the leachables released from the tested scaffolds can be considered as noncytotoxic.

Cell Viability by MTS and Calcein-AM Staining. Results showed that the tested hBMSCs were also able to reduce MTS (Figure 2), demonstrate high metabolic rates as a function of time, and denote a high viability and proliferation profile. Moreover, a cell viability assay with calcein-AM staining (Figure 3) demonstrated that hBMSCs were metabolically active and well distributed throughout the scaffold surfaces after 3 weeks.

Cell Adhesion and Morphology by SEM. After 1 week, hBMSCs cultured under osteogenic conditions, were able to adhere to the fibrous surface and inner pores of the scaffolds and to proliferate during the subsequent periods in culture (Figure 4A,D,G). The production of ECM can be analyzed in more depth at higher magnifications (Figure 4C,F,I). Furthermore, it is observed that the cells were able to create "bridges" between neighboring fibers, but without occluding the pores (Figure 4B,E). Cells were also capable of colonizing the inner regions of the scaffolds, keeping the viability on those inner pores (Figure 4J,K,L).

Alkaline Phosphatase Quantification. The expression of ALP is typically used as an early marker of the osteogenic phenotype. The ALP expression shows the typical pattern of expression (Figure 5) increasing until the second week, where it reached its maximum. This observation reflects the early osteogenic differentiation stage of the MSCs. After this period, ALP activity decreased, probably due to the onset of the mineralization process.[39] This observation is a positive indication of the transient character of the differentiation of cells into the osteogenic lineage.

Mineralization Content of ECM by EDS and FTIR Analysis. EDS analysis of the surface of cell-constructs detected the presence of Ca and P elements (Figure 6A). Acellular scaffolds (control) do not show any presence of those two

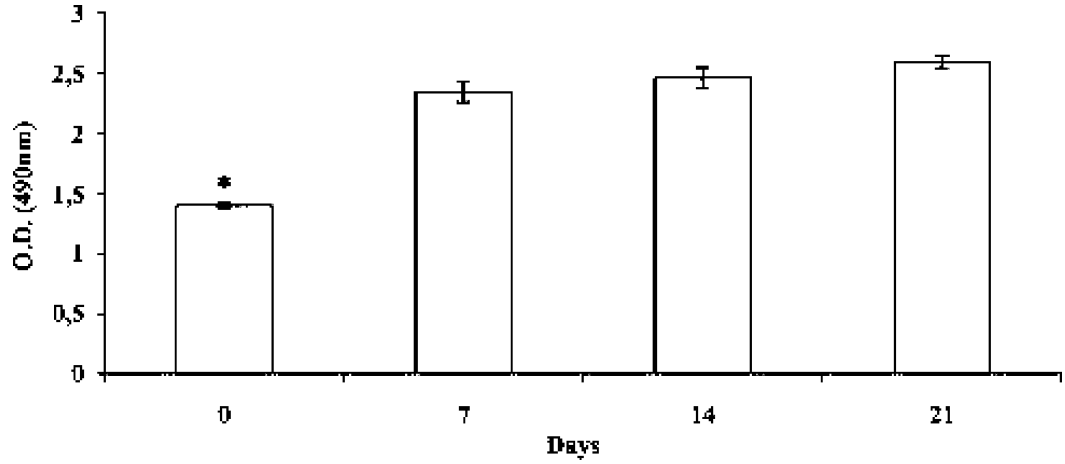

Figure 2. MTS viability assay of cell-constructs and cultured Ch-PBS scaffolds following 3 h (0 days), 7, 14, and 21 days after cell seeding. Results are expressed as means ± standard deviation with $n = 3$ for each bar; (*) indicates a significant difference ($p < 0.05$) between testing conditions as a function of time.

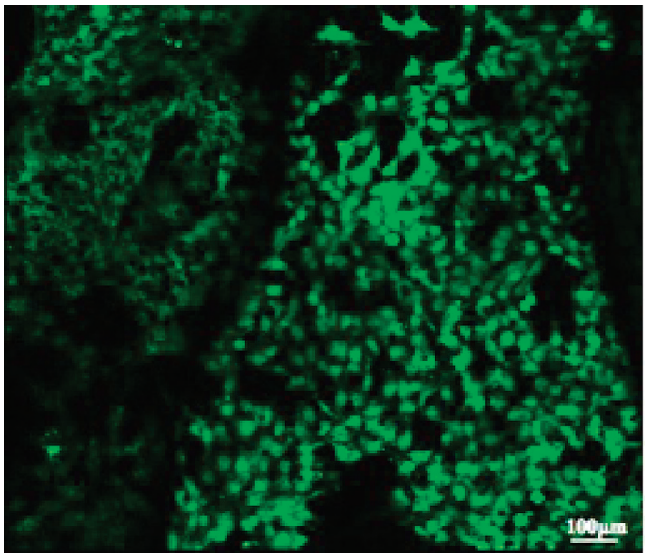

Figure 3. Cell viability after three weeks of cell-culture in the scaffolds analyzed by calcein-AM staining. Confocal micrograph showing cell adhesion and viability on the Ch-PBS fiber mesh scaffolds after 3 weeks in culture.

elements during the same period of immersion in osteogenic inducing culture medium. These results clearly indicate the formation of mineralized ECM at the surface of cell seeded scaffolds. These results were further confirmed by FTIR analysis (Figure 6C), showing the presence of phosphate and carbonate groups, which are typical for carbonated apatite.[41]

Osteogenic Differentiation of hMSCs upon Chitosan-Based Scaffolds. To further analyze the differentiation toward the osteogenic phenotype, the RNA of the cell cultured in the scaffolds is analyzed by reverse transcriptase PCR (Figure 7).

PCR analysis shows the expression of specific genes related to the osteogenic lineage, namely, the transcription factor Runx2, considered to be a crucial transcription gene within the osteogenic phenotype.[42,43] Its expression was detected at all time points, being more pronounced at the third week of culture. The gene expression patterns of the various extracellular proteins, including osteocalcin, type 1 collagen, and BSP, was detected at all time points and in increased levels at the latest time point. This indicates a successful differentiation into the osteogenic phenotype.

Discussion

The demand for new therapies for diseases affecting musculoskeletal tissues is continuously increasing, especially considering the high number of patients suffering from skeletal degenerative diseases. Bone tissue engineering has been proposing solutions to address those clinical problems. The strategy could combine cells with a 3D scaffold and growth factors, seeking to achieve the regeneration of bone tissue.

Natural-based polymers such as chitosan, a polymer produced by partial deacetylation of chitin, have been proposed as having potential for tissue engineering applications. Chitosan is characterized by its good biocompatibility, low immunogeneicity, noncytotoxicity and wound healing capability. These properties make chitosan a strong candidate material for bone tissue engineering applications. Due to its limited mechanical properties and process ability, scaffolds produced only with chitosan are more difficult to optimize for hard tissue applications. An alternative methodology to overcome those limitations consists in blending chitosan with synthetic and biodegradable aliphatic polyesters.[23,30] Thermoplastic biodegradable polymers have already shown great potential in the clinic as implantable biomaterials due to their reported noncytotoxicity and biodegradability. Their degradation products are also noncytotoxic, although they lack the cell recognition affinity typically provided by natural polymers. Thus, by blending chitosan with synthetic polyesters, it is possible to obtain a good balance between biological affinity[27−29] and processability, not compromising the biodegradability.

The developed fibrous scaffolds showed a significant interconnectivity (Figure 1), which is known to be a critical condition for successful cell colonization and viability. Extracts from the developed scaffolds are noncytotoxic in contact with L929 cells (data not presented herein).

Human MSCs showed high metabolic levels when adhered onto the scaffolds both by the reduction of the MTS substrate (Figure 2) and also by the calcein-am staining (Figure 3).

SEM micrographs (Figure 4) show that hBMSCs adhered at the surface of the scaffolds and were able to "bridge" between fibers without occluding the pores (Figure 4C). The proliferation of hBMSCs and the production of ECM showed increased levels over time (Figure 4A,D,G). SEM observations and cell viability results can help to establish a time-dependent cell proliferation pattern as showing the presence of higher number of cells at late time periods. It was also observed that cells proliferated

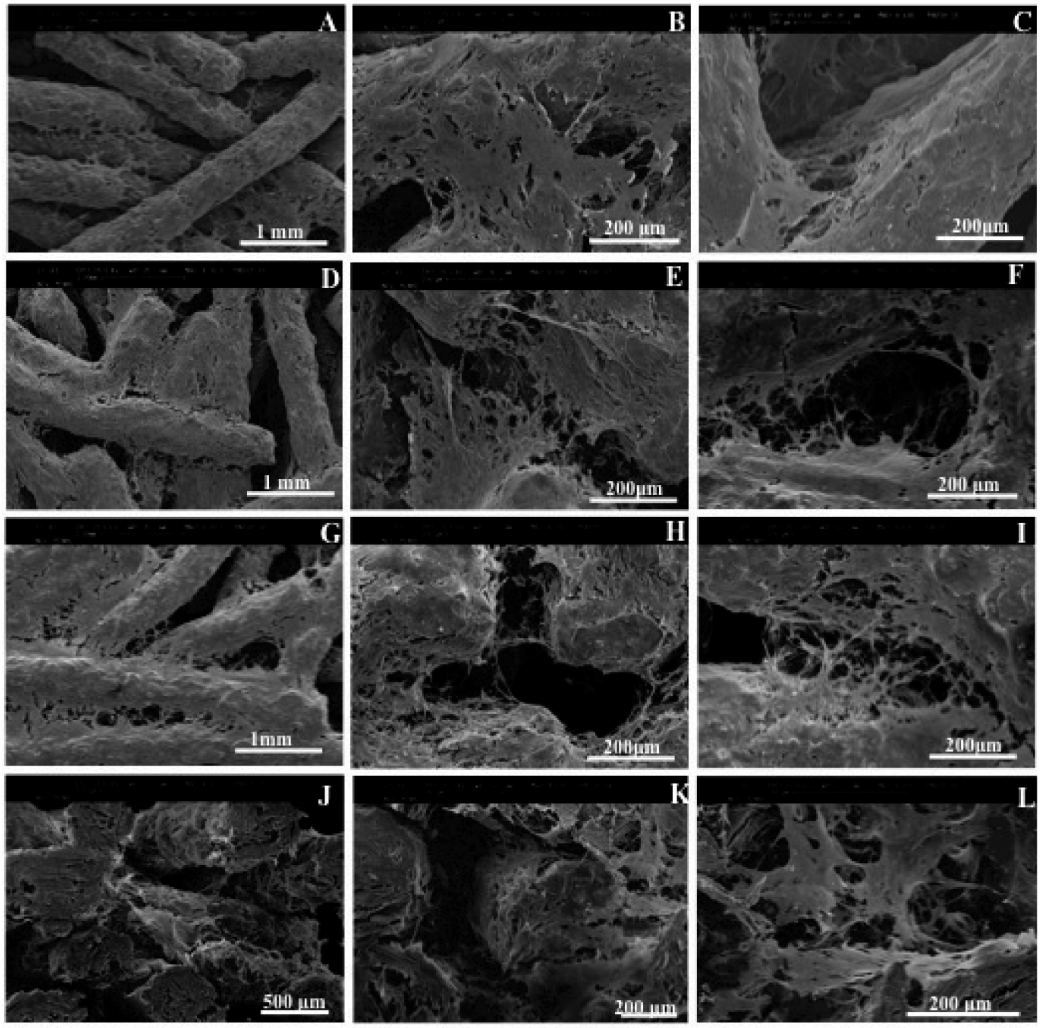

Figure 4. SEM micrographs of the adhesion and proliferation of hBMSCs, under osteogenic induction, on the 50% wt Ch-PBS fiber mesh scaffolds at the surface after 1 week (A, B, C), 2 weeks (D, E, F), and 3 weeks (G, H, I). The micrographs J, K, and L correspond to cross sections of the cell seeded scaffolds after 3 weeks, showing the bulk colonization by the cells.

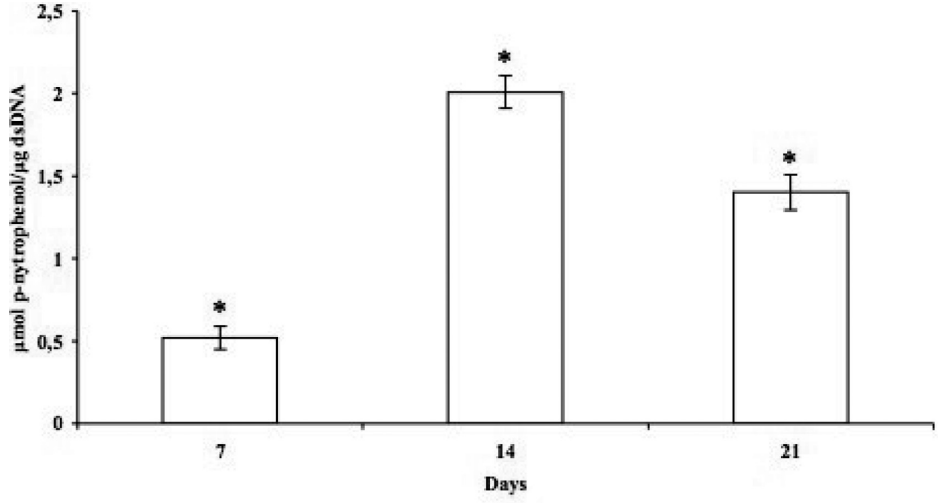

Figure 5. Alkaline phosphatase activity of hBMSCs cultured on the scaffolds at time points 1, 2, and 3 weeks, under osteogenic induction. The results are normalized by μg of dsDNA and presented in amount of *p*-nitrophenol (μmol/mL/h/μg dsDNA). Results are expressed as average $\pm$ standard deviation with $n = 3$ for each bar, (*) indicates a significant difference ($p < 0.05$) between conditions as a function of time.

and colonized the inner regions (Figure 4J−L) of the scaffolds, which demonstrate that porosity and interconnectivity exhibited by the scaffolds are adequate for cell infiltration and ingrowth.

ALP activity measurements (Figure 5) showed a maximum at the second week of culture, reflecting the early osteogenic differentiation stage of hMSCs.[39] After this period, ALP activity decreased due to the onset of the mineralization process, which is a typical positive indication.

hBMSCs were able to produce mineralized ECM confirmed by the presence of Ca and P elements (Figure 6a). Furthermore,

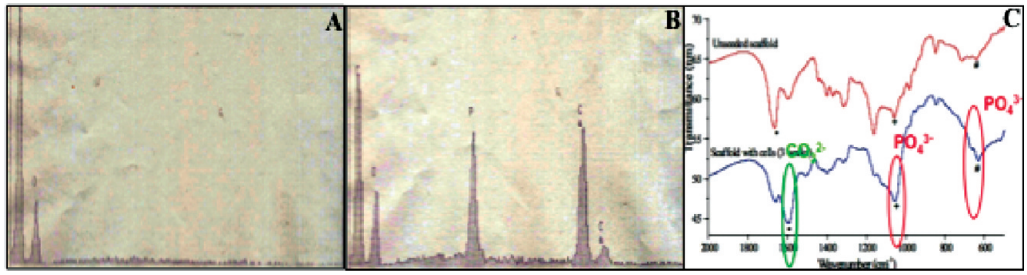

Figure 6. EDS spectra of the acellular scaffolds (A), 3 weeks in culture of hBMSCs on Ch-PBS scaffolds (B), and FTIR spectra of the control and cell-constructs (C; $*CO_3^{2-}$, + # PO_4^{3-}).

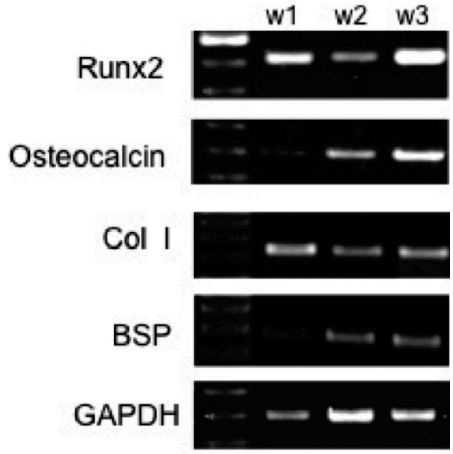

Figure 7. PCR analysis of the genes that encode for the transcription factor Runx2, the bone ECM protein osteocalcin, type I collagen, bone sialoprotein (BSP), and the house-keeping gene GAPDH on hBMSCs grown under osteogenic conditions on Ch-PBS fiber mesh scaffolds for 21 days.

the existence of characteristic peaks of carbonate and phosphate groups in FTIR spectra (Figure 6C) indicates the presence of carbonated apatite at the surface of cell-constructs.

The differentiation of the hBMSCs toward the osteogenic lineage was ultimately demonstrated by the expression of genes that are usually associated with the mineralization during osteogenesis, such as the transcription factor Runx2, and the matrix proteins osteocalcin, type 1 collagen, and BSP (Figure 7). Runx2 is essential for the differentiation of MSCs into mature osteoblasts in the skeletal development of numerous mammalian organisms.[42,43] Osteocalcin, one of the few osteogenic specific genes, is a bone matrix protein and is known to play an important role in the differentiation of osteoblast progenitor cells, with significant up-regulation observed both in matrix synthesis and in the mineralization process.[43] BSP is secreted, bind cell surface integrin receptors, and regulate mineralization, and type I collagen represents the majority of the organic part of bone matrix.[44]

Conclusions

Chitosan-poly(butylene succinate) fiber mesh scaffolds were successfully produced by a melt based routine, avoiding the use of solvents. The scaffolds presented a high degree of interconnectivity (89.6% ± 1.9) and adequate mechanical properties (32.6 ± 12.8 MPa) for bone tissue engineering applications.

It was demonstrated that chitosan-PBS scaffolds are cytocompatible, both with L929 cells and hBMSCs. The scaffolds support hBMSCs adhesion and proliferation under osteogenic inducing conditions. The cells presented high levels of viability, demonstrating that besides the remarkable colonization of the scaffold structure, the cells were metabolically active.

ALP expression an mineralized ECM is detected by the presence of Ca and P elements in EDS spectra and also confirmed by FTIR. The expression of osteogenic related genes (Runx2, osteocalcin, type 1 collagen and bone sialoprotein) show successful differentiation of the cells in the scaffolds toward an osteogenic phenotype.

Due to the extremely well balanced combination of properties and excellent biological performance, it is strongly believed that the scaffolds herein proposed in combination with human adult mesenchymal stem cells will provide new therapies for the development of tissue engineering solutions for bone regeneration.

Acknowledgment. Ana Costa-Pinto was supported by a grant (SFRH/24735/2005) from the Portuguese Foundation for Science and Technology "Fundação para a Ciência e a Tecnologia" (FCT). This work was partially supported by the EU Integrated Project GENOSTEM (Adult Mesenchymal Stem Cells Engineering for connective tissue disorders: from the bench to the bedside, LSHB-CT-2003-5033161), and the European Network of Excellence EXPERTISSUES (NMP3-CT-2004-500283). The authors would like to acknowledge to the School of Health Sciences of the University of Minho for the opportunity of using its facilities.

Supporting Information Available. The primers used are described in Table 1 and the results concerning the cytotoxicity results of the 72 h extracts of the chitosan-PBS fiber mesh scaffolds, (Figure 1) and the DNA quantification results of the hBMSCs cultured under osteogenic conditions onto Ch-PBS scaffolds (Figure 2) are provided. This material is available free of charge via the Internet at http://pubs.acs.org.

References and Notes

(1) Friedenstein, A. J.; Deriglasova, U. F.; Kulagina, N. N.; Panasuk, A. F.; Rudakowa, S. F.; Luriá, E. A.; Ruadkow, I. A. *Exp. Hematol.* **1974**, *2*, 83–92.
(2) Owen, M. *J. Cell. Sci. Suppl.* **1988**, *10*, 63–76.
(3) Bianco, P.; Robey, P. G. *J. Clin. Inv.* **2000**, *105*, 1663–1668.
(4) Bianco, P.; Robey, P. G. *Nature* **2001**, *1*, 118–121.
(5) Delorme, B.; Ringe, J.; Pontikoglou, C.; Gaillard, J.; Langonné, A.; Sensebé, L.; Noël, D.; Jorgensen, C.; Häupl, T.; Charbord, P. *Stem Cells* **2009**, *27*, 1142–1151.
(6) Giannoudis, P. V.; Dinopoulos, H.; Tsiridis, E. *Int. J. Care Injured* **2005**, *36*, 20–27.
(7) Salgado, A. J.; Coutinho, O. P.; Reis, R. L. *Macromol. Biosci.* **2004**, *4*, 743–745.
(8) Langer, R.; Vacanti, J. *Science* **1993**, *260*, 920–925.
(9) Cancedda, R. *Matrix Biol.* **2003**, *22*, 81–91.
(10) Hutmacher, D. H.; Schantz, J. T.; Lam, C. F. X.; Tan, K. C.; Lim, T. C. *J. Tissue Eng. Regen. Med.* **2007**, *1*, 245–260.
(11) Reis, R. L.; Cunha, A. M. *J. Mater. Sci.: Mater. Med.* **1995**, *6*, 786–792.

(12) Mendes, S. C.; Reis, R. L.; Bovell, Y. P.; Cunha, A. M.; van Blitterswijk, C. A.; de Bruijn, J. D. *Biomaterials* **2001**, *22*, 2057–2064.
(13) Salgado, A. J.; Gomes, M. E.; Chou, A. M.; Coutinho, O. P.; Reis, R. L.; Hutmacher, D. W. *Mater. Sci. Eng., C* **2002**, *20*, 27–33.
(14) Alves, C. M.; Reis, R. L.; Hunt, J. A. *J. Mater. Sci.: Mater. Med.* **2003**, *14*, 157–165.
(15) Gomes, M. E.; Sikavitsas, V. I.; Behravesh, E.; Reis, R. L.; Mikos, A. G. *J. Biomed. Mater. Res., Part A* **2003**, *67*, 87–95.
(16) Salgado, A. J.; Coutinho, O. P.; Reis, R. L. *Tissue Eng.* **2004**, *10*, 465–474.
(17) Leonor, I. B.; Kim, H. M.; Balas, F.; Kawashita, M.; Reis, R. L.; Kokubo, T.; Nakamura, T. *J. Tissue Eng. Regen. Med.* **2007**, *1*, 425–435.
(18) Gomes, M. E.; Azevedo, H. S.; Moreira, A. R.; Ellä, V.; Kellomäki, M.; Reis, R. L. *J. Tissue Eng. Regen. Med.* **2008**, *2*, 243–252.
(19) Oliveira, J. M.; Rodrigues, M. T.; Silva, S. S.; Malafaya, P. B.; Gomes, M. E.; Reis, R. L. *Biomaterials* **2006**, *27*, 6123–6137.
(20) Madihally, S. V.; Matthew, H. W. T. *Biomaterials* **1999**, *20*, 1133–1142.
(21) Kumar, M. N. V. R. *React. Funct. Polym.* **2000**, *46*, 1–27.
(22) Martins, A. M.; Santos, M. I.; Azevedo, H. S.; Malafaya, P. B.; Reis, R. L. *Acta Biomater.* **2008**, *4*, 1637–1645.
(23) Correlo, V. M.; Boesel, L. F.; Bhattacharya, M.; Neves, N. M.; Reis, R. L. *Mater. Sci. Eng., A* **2005**, *403*, 57–68.
(24) Correlo, V. M.; Boesel, L. F.; Bhattacharya, M.; Neves, N. M.; Reis, R. L. *Macromol. Mater. Eng.* **2005**, *290*, 1157–1165.
(25) Correlo, V. M.; Pinho, E. D.; Pashkuleva, I.; Bhattacharya, M.; Neves, N. M.; Reis, R. L. *Macromol. Biosci.* **2007**, *7*, 354–363.
(26) Correlo, V. M.; Boesel, L. F.; Pinho, E. D.; Costa-Pinto, A. R.; Alves da Silva, M.; Bhattacharya, M. Mano, J. F.; Neves, N. M.; Reis R. L. *J. Biomed. Mater. Res., Part A* **2008**, doi: 10.1002/jbm.a.32221.
(27) Coutinho, D. F.; Pashkuleva, I. H.; Alves, C. M.; Marques, A. P.; Neves, N. M.; Reis, R. L. *Biomacromolecules* **2008**, *9*, 1139–1145.
(28) Costa-Pinto, A. R.; Correlo, V. M.; Sol, P. C.; Battacharya, M.; Charbord, P.; Delorme, B.; Reis, R. L.; Neves, N. M. *Tissue Eng., Part A* **2008**, *14*, 1049–1057.
(29) Oliveira, J. T.; Correlo, V. M.; Sol, P. C.; Costa-Pinto, A. R.; Malafaya, P. B.; Salgado, A. J.; Bhattacharya, M.; Charbord, P.; Neves, N. M.; Reis, R. L. *Tissue Eng., Part A* **2008**, *14*, 1651–61.
(30) Correlo, V. M.; Costa-Pinto, A. R.; Sol, P. C.; Covas, J. A.; Bhattacharya, M.; Neves, N. M.; Reis, R. L. manuscript in preparation.
(31) Petillo, O.; Ranieri, M.; Santin, M.; Ambrosia, L.; Calabró, D.; Avallone, B.; Balsamo, G. *Biomaterials* **1994**, *15*, 1215–1220.
(32) VandeVord, P. J.; Matthew, H. W.; DeSilva, S. P.; Mayton, L.; Wu, B.; Wooley, P. H. *J. Biomed. Mater. Res., Part A* **2002**, *59*, 585–590.
(33) Lee, J. Y.; Park, J. Y.; Lee, Y. M.; Ku, Y.; Rhyu, I. C.; Lee, S. J.; Han, S. B.; Chung, C. P. *Biotechnol. Lett.* **2004**, *26*, 1037–1041.
(34) Tuzlakoglu, K.; Alves, C. M.; Mano, J. F.; Reis, R. L. *Macromol. Biosci.* **2004**, *4*, 811–819.
(35) Chatelet, C.; Damour, O.; Domard, A. *Biomaterials* **2001**, *22*, 261–268.
(36) Heinemann, C.; Heinemann, S.; Bernhardt, A.; Worch, H.; Hanke, T. *Biomacromolecules* **2008**, *10*, 2913–2920.
(37) Delorme, B.; Charbord, P. *Methods Mol. Med.* **2007**, *140*, 67–81.
(38) Bray, D. F.; Bagu, J.; Koegler, P. *Microsc. Res. Tech.* **1993**, *26*, 489–495.
(39) Maniatopoulos, C.; Sodek, J. M.; Melcher, A. H. *Cell Tissue Res.* **1988**, *254*, 317–330.
(40) Yang, S.; Leong, K.; Zu, D. O.; Chua, C. *Tissue Eng.* **2001**, *7*, 679–689.
(41) Rehman, I.; Bonfield, W. J. *Mater. Sci.: Mater. Med.* **1997**, *8*, 1–4.
(42) Lian, J. B.; Stein, G. S. *Curr. Pharm. Des.* **2003**, *9*, 2677–2685.
(43) Viereck, V.; Siggelkow, H.; Tauber, S.; Raddatz, D.; Schutze, N.; Hufner, M. J. *Cell Biochem.* **2002**, *86*, 348–356.
(44) Liu, F.; Akiyama, Y.; Tai, S.; Maruyama, K.; Kawaguchi, Y.; Muramatsu, K.; Yamaguchi, K. *J. Bone Miner. Metab.* **2008**, *26*, 312–320.

BM9000102